

An Analytically Solvable Model of Firing Rate Heterogeneity in Balanced State Networks

Alexander Schmidt^{1,3}, Peter Hiemeyer¹, and Fred Wolf^{1-6*}

¹Max Planck Institute for Dynamics and Self-Organization, Göttingen, Germany

²Göttingen Campus Institute for Dynamics of Biological Networks, University of Göttingen, Göttingen, Germany

³Max Planck Institute for Multidisciplinary Sciences, Göttingen, Germany

⁴Institute for the Dynamics of Complex Systems, University of Göttingen, Göttingen, Germany

⁵Center for Biostructural Imaging of Neurodegeneration, Göttingen, Germany and

⁶Bernstein Center for Computational Neuroscience Göttingen, Göttingen, Germany

Distributions of neuronal activity within cortical circuits are often found to display highly skewed shapes with many neurons emitting action potentials at low or vanishing rates, while some are active at high rates. Theoretical studies were able to reproduce such distributions, but come with a lack of mathematical tractability, preventing a deeper understanding of the impact of model parameters. In this study, using the Gauss-Rice neuron model, we present a balanced-state cortical circuit model for which the firing rate distribution can be exactly calculated. It offers selfconsistent solutions to recurrent neuronal networks and allows for the combination of multiple neuronal populations, with single or multiple synaptic receptors (e.g. AMPA and NMDA in excitatory populations), paving the way for a deeper understanding of how firing rate distributions are impacted by single neuron or synaptic properties.

I. INTRODUCTION

Spikes are the principal currency of information flow in the cerebral cortex, but cortical neurons differ strongly in the amount of this currency they are handing out per time unit. In general, firing rates in *bona fide* uniform populations of cortical principal neurons vary widely and often exhibit highly skewed distributions both in spontaneous and in driven states [1–10]. It is well understood that broad and skewed firing rate distributions are a generic and robust property in models of recurrently connected networks of cortical neurons [11–18]. In particular, in balanced state networks broad and skewed firing rate distributions even emerge in situations of uniform external drive. This results because most inputs to individual neurons originate from other neurons within the cortical circuit, making the total input subject to heterogeneities in the composition of cortical presynaptic cells and the total number of received synapses [11, 12]. Together with the approximate balancing of excitation by

feedback inhibition, this generically leads to the emergence of broad and skewed firing rate distributions.

The shape and range of the emerging firing rate distribution, in general, is determined by a set of self-consistency requirements [11, 12]. In essence, inputs drawn from the correct firing rate distribution must drive the postsynaptic cells in the network to fire at rates that agree with the assumed firing rate distribution. For balanced state networks on random graphs, these conditions can be expressed mathematically by a few self-consistency equations that become exact in the large system limit. Prior work indicates that these equations are sensitive to a variety of network parameters, from synaptic efficiencies and connection probabilities to single neuron f-I-curves and the dynamics of synaptic inputs [11–18]. These seminal studies conclusively demonstrated that the emergence of realistic firing rate distributions is a robust feature of such networks. Due to the complexity of the dependencies on biological detail and a lack of mathematical tractability of the self-consistency equations, the impact of synaptic and network parameters on the shape and range of firing rate distributions is not sufficiently understood.

Utilizing the superior mathematical tractability of the Gauss-Rice neuron model, we here introduce a balanced-state cortical circuit model for which the firing rate distribution can be exactly calculated. We find that the self-consistency equations determining the shape and position of the firing rate distribution take the form of relatively simple transcendental equations that can be easily solved. The emergent firing rate distribution is determined by a small number of effective parameters that capture the dependence of the rate distribution on the cellular and synaptic properties in the network. In particular, we treat the case of a local circuit composed of excitatory and inhibitory neurons in which excitatory synaptic currents exhibit different decay times reflecting for instance a mixture of AMPA and NMDA receptors at individual synapses.

* fred.wolf@ds.mpg.de

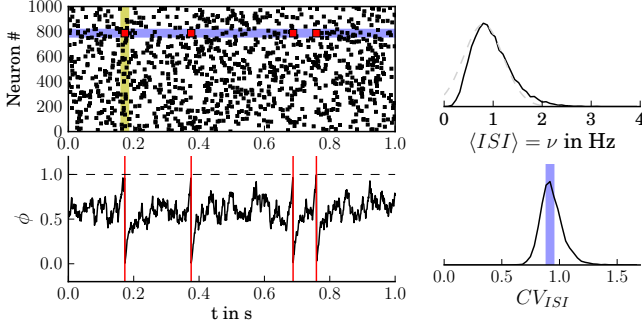


FIG. 1. Asynchronous, irregular spiking activity in the Balanced State; top left: spike raster of a network. Irregular spiking activity of one neuron over time is highlighted by the blue bar while the yellow bar highlights the asynchronous activity over the network at a random timepoint; bottom left: phase trace of the highlighted neuron; top right: the firing rate distribution has a characteristic shape with a peak at low rates and some skewness (grey dashed gaussian as reference); bottom right: Irregular firing is indicated by a CV value distribution peaked close to one

II. METHODS

A. Network topology and setup

We consider a network defined by a directed Erdős-Rényi graph with first order connectivity $p = K/N$, where K is the average number of connections per neuron and N the total number of neurons in the network. The limit $1 \ll K \ll N$, with $N, K \rightarrow \infty$, allows for a mean-field approach when modeling network dynamics.

The connectivity is described by an $N \times N$ -matrix with entries A_{kl}^{ij} that encode the connections of neuron j of population l to neuron i of population k . The population indices k and l point to regions of the connectivity matrix, that refer to the respective population and that follow statistics based on their identity. The indices i and j run only over their respective populations. Differences in absolute numbers of synaptic connections between the populations can be captured by the factor κ_l . $A_{kl}^{ij} = 1$ if there is a connection and 0, otherwise. The mean outward connectivity of population l is obtained as

$$[A_{kl}^{ij}]_{ijk} = \sum_{k=EI} \frac{1}{N_k} \sum_{i=1}^{N_k} \frac{1}{N_l} \sum_{j=1}^{N_l} A_{kl}^{ij},$$

which is an average over all presynaptic neurons of population l and all postsynaptic neurons in the network. It yields $[A_{kl}^{ij}]_{ijk} = \kappa_l \frac{K}{N}$.

A stationary state with temporal fluctuations independent of network size is obtained by scaling the synaptic weights according to [11, 12, 19]:

$$\tilde{J}_{kl} = \pm \frac{J_{kl}}{\sqrt{K}}, \quad J_{kl} > 0. \quad (1)$$

Interactions between neurons are mediated by electrical signals (action potentials or *spikes*) inducing post-synaptic currents (PSCs), that can be of either inhibitory (negative synaptic weight in eq. 1, $l = I$) or excitatory (positive weight, $l = E$) nature. According to Dale's Principle, our model neurons can only have one kind of impact on its postsynaptic neurons, allowing for a clear distinction of two populations in the network: an excitatory (E) and an inhibitory (I) one.

We describe PSCs by a normalized kernel of shape

$$f_l(t - t^{(p)}) = \sum_m \frac{r_{l_m}}{\mathcal{N}_{l_m}} \exp\left(-\frac{t - t^{(p)}}{\tau_{l_m}}\right) \Theta(t - t^{(p)}) \quad (2)$$

$$\sum_m r_{l_m} = 1, \quad \mathcal{N}_{l_m} \in [1, \tau_{l_m}]$$

where Θ is the Heavyside-function and $t^{(p)}$ the time of a spike. Our model allows for multiple types of post-synaptic receptors, including mixtures with different temporal characteristics: τ_{l_m} is the m th synaptic time-constant of population l , e.g. inhibitory (GABAergic, few ms decay time, [20, 21]) or fast (AMPA, few ms, [22]) and slow (NMDA, several 100 ms, [22, 23]) excitatory ones. The mixture parameters r_{l_m} specify the fraction of each type of receptor per synapse and the normalization constant \mathcal{N}_{l_m} specifies, whether the kernel is normalized with respect to the total deposited charge ($= \tau_{l_m}$), or to its peak current ($= 1$). In the limit $\tau_l \rightarrow 0$ one would obtain δ -pulses, effectively resulting in an Ornstein-Uhlenbeck process membrane potential process.

For simplicity, we first assume *pure* kernels first, with a single post-synaptic receptor type:

$$f_l(t - t^{(p)}) = \frac{1}{\mathcal{N}_l} \exp\left(-\frac{t - t^{(p)}}{\tau_{l_i}}\right) \Theta(t - t^{(p)}), \quad (3)$$

and later treat the case of mixed receptors in Sec. IID

We assume uniform synaptic weights and kernels of the PSCs for all neurons within a population and finally drive the network by a population-specific, external constant excitatory current I_k^{ext} .

As we will show below, this setup allows calculating of quenched and dynamic fluctuations of inputs across the network (at any given time) once the compound spike train statistics are determined (Fig. 2(c)).

B. Input current statistics

1. Compound spike train statistics

The temporal sequence of spikes from a single neuron constitutes a point process [19, 24, 25], termed *spike train*. The entirety of incoming spikes to neuron i is the *compound spike train* with rate

$$\Omega_i(t) = \sum_{j \in \text{pre}(i)} \nu_j(t), \quad (4)$$

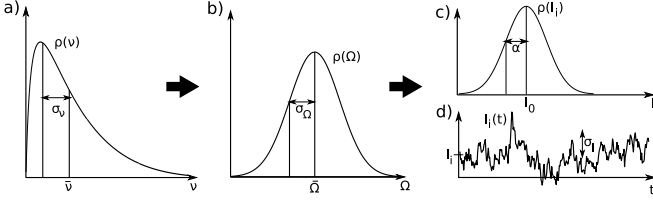


FIG. 2. Spike train- and input current statistics are derived from the firing rate distribution; (a) probability density function (pdf) of firing rates across neurons $\rho(\nu)$; (b) pdf of compound spike rate Ω ; (c) input current distribution (mean and quenched variance marked); (d) temporal fluctuations of input current governed by the shape of the PSC-kernel

where $\text{pre}(i)$ is the set of presynaptic neurons to neuron i ($A_{kl}^{ij} = 1$). Individual firing rates ν_j are sampled from an underlying, yet unknown firing rate distribution (Fig. 2(a)), which is to be selfconsistently derived. Due to $N \rightarrow \infty$ and the sparse connectivity ($N \gg K$) presynaptic neuronal activity is uncorrelated [16] and the compound spike train can be approximated as a Poisson-like point process, even if individual cells' activity deviates from this simple statistics. Large K by application of the central limit theorem implies the total recurrent synaptic current to be Gaussian. Accordingly, the *Compound spike train statistics* (Fig. 2(b)) are sufficiently described by their first and second moment.

In the stationary case the spike train of each presynaptic neuron $\text{pre}(i)$ contributes on average ν APs per second to the Poissonian compound spike rate Ω_i (eq.4) with the network average:

$$\begin{aligned} \Omega &= [\Omega_i]_i = \sum_{l=E,I} [\Omega_l^i]_i \\ &= \sum_{l=E,I} \left[\sum_{j=1}^{N_l} A_{kl}^{ij} \nu_l^j \right]_i = \sum_{l=E,I} N_l [A_{kl}^{ij}]_{ij} [\nu_l^j]_j \\ &= \sum_{l=E,I} N_l \kappa_l \frac{K}{N_l} \bar{\nu}_l = K(\kappa_E \bar{\nu}_E + \kappa_I \bar{\nu}_I), \end{aligned} \quad (5)$$

where $[\cdot]_i$ denotes the network average over postsynaptic neurons i and we used the statistical independence of presynaptic firing rates ν_l^j and the matrix entries A_{kl}^{ij} . The second moment $[\Omega_i^2]_i$ and thus the resulting variance over the network $\text{Var}(\Omega) = [\Omega_i^2]_i - [\Omega_i]^2$ evaluates to (see App.A 1):

$$\text{Var}(\Omega) = K(\kappa_E q_E + \kappa_I q_I), \quad (6)$$

where q_l denotes the second moment of the firing rate distribution of population l . This concludes the calculations of the statistics of the compound spike train statistics, Fig. 2(b)

2. Time-averaged (quenched) input current statistics

Each realization of a spike train is described by a set of spike times $\{t^{(p)}\}$ that lead to postsynaptic current $I_i(t | \{t^{(p)}\}) = J_{kl} f_l(t - t^{(p)})$. The total current to neuron i is

$$I_i(t | \{t^{(p)}\}) = J \sum_{l=E,I} \sum_{j=1}^{N_l} A_{kl}^{ij} \sum_{p=1}^{N_{AP}} f_l(t - t^{(p)}).$$

Here we denote the total number of spike times $t^{(p)}$ within the interval $t \in [0, T]$ in one compound spike train as N_{AP} . The probability of any realizations of such a spike train with rate $\Omega(t)$ is [26]

$$P(\{t^{(p)}\} | \Omega(t)) = \frac{e^{-\int_0^T dt \Omega(t)}}{N_{AP}!} \prod_{p=1}^{N_{AP}} \Omega(t^{(p)}).$$

We obtain the total current into neuron i using the independence of subsequent PSCs, allowing us to integrate over the N_{AP} -dimensional hypercube, covering the temporal course of one spike per dimension.

Accounting for the complete space of possible realization of compound spike trains, we average over all $N_{AP} \in \mathbb{N}$. Assuming stationarity, the average input current evaluates to (see App. A 2):

$$\langle I_k^i(t) \rangle = \frac{1}{\sqrt{K}} \sum_{l=E,I} J_{kl} f_{N_l} \Omega_l^i, \quad (7)$$

f_{N_l} being the integral evaluated over the kernel of population l .

The linear dependence on the compound spike rate allows to determine the mean and quenched variance from the statistics of Ω from Eq. 5 and 6:

$$\bar{I}_k^{\text{rec}} := [\langle I_k^i(t) \rangle]_i = \sqrt{K} f_{N_l} (J_{kE} \kappa_E \bar{\nu}_E - J_{kI} \kappa_I \bar{\nu}_I) \quad (8)$$

$$\begin{aligned} \alpha_{I_k}^2 &:= [(\langle I_k^i(t) \rangle - \bar{I}_k^{\text{rec}})^2]_i = \sum_{l=E,I} \frac{J_{kl}^2}{K} f_{N_l}^2 \text{Var}(\Omega_l^i) \\ &= J_{kE}^2 f_{N_E} \kappa_E q_E + J_{kI}^2 f_{N_I} \kappa_I q_I \end{aligned} \quad (9)$$

Note, that the scaling of synaptic weights (Eq. 1) keeps the quenched variance independent of network size. Network- and time-averaged input currents follow a scaling with $K^{\frac{1}{2}}$, while individual neurons' temporal averages of input currents deviate from this according to a Gaussian distribution with variance $\alpha_{I_k}^2$ (c.f. Fig. 2(c)).

3. Temporal input current statistics

Additional to the neuron-to-neuron differences in quenched input current, we obtained the temporal fluctuations. The statistics of input currents originating from population l can be captured by the covariance function,

App. A 2 b:

$$C_{I_{kl}^i}(t, t') := \frac{J_{kl}^2 \Omega_l^i}{K} \int_{-\infty}^{\infty} ds f_I(s-t) f_I(s-t')$$

Evaluating the integral with the defined PSC-kernel (Eq. 3) and substituting $\Delta t = t - t'$:

$$C_{I_{kl}^i}(\Delta t) = \frac{J_{kl}^2 \Omega_l^i}{K} \frac{\tau_{I_l}}{2\mathcal{N}_l^2} \exp\left(-\frac{|\Delta t|}{\tau_{I_l}}\right) \quad (10)$$

$$\sigma_{I_{kl}^i}^2 = C_{I_{kl}^i}(0) = \frac{J_{kl}^2 \Omega_l^i \tau_{I_l}}{2K\mathcal{N}_l^2} \quad (11)$$

The mean and variance of σ_{I_i} can be obtained from the compound spike trains statistics (Eq. 5, 6):

$$\sigma_{I_k}^2 = \sum_{l=E,I} \sigma_{I_{kl}^i}^2 = \sum_{l=E,I} \kappa_l \frac{J_{kl}^2 \bar{\nu}_l \tau_{I_l}}{2\mathcal{N}_l} \quad (12)$$

$$\begin{aligned} \text{Var}_k^i(\sigma_{I_k}^2) &= \sum_{l=E,I} \frac{J_{kl}^4 \tau_{I_l}^2}{4K^2 \mathcal{N}_l^4} \text{Var}(\Omega_l^i) \\ &= \frac{1}{K} \sum_{l=E,I} \frac{J_{kl}^4 \tau_{I_l}^2}{4\mathcal{N}_l^4} q_l \xrightarrow{K \rightarrow \infty} 0 \end{aligned} \quad (13)$$

As expected from the scaling of synaptic weights (Eq. 1), the variance of the temporal fluctuations in large networks is independent of network size ($\text{Var}(\sigma_I^2) \rightarrow 0$). All neurons are thus subject to statistically identical temporal fluctuations with variance σ_I^2 . We have thus concluded obtaining all parameters describing the temporal fluctuations, sketched in Fig. 2(d).

4. Overall distribution of input currents

Summarizing the different internal (\bar{I}^{rec} , α_I , σ_I) and external (I^{ext}) components of the input current to a single neuron i in population k , we obtain:

$$\begin{aligned} I_k^i(t) &= \overbrace{\sqrt{K}(I_k^{ext} + J_{kE} f_{N_E} \kappa_E \bar{\nu}_E - J_{kI} f_{N_I} \kappa_I \bar{\nu}_I)}^{=: \bar{I}_k^0, \text{ network \& time averaged}} \\ &\quad + \underbrace{\alpha_{I_k} x_i}_{\text{network var.}} + \underbrace{\sigma_{I_k} \eta_i(t)}_{\text{temporal var.}}, \end{aligned} \quad (14)$$

where x_i is a Gaussian random number with 0 mean and variance 1. The temporal course is described by the stochastic function $\eta_i(t)$. Dropping the neuron index i for readability, the temporal average $\bar{I}_k = \langle I_k(t) \rangle_t$ is distributed across the network as:

$$\rho(\bar{I}_k) = \frac{1}{\sqrt{2\pi\alpha_{I_k}^2}} \exp\left(-\frac{(\bar{I}_k - \bar{I}_k^0)^2}{2\alpha_{I_k}^2}\right) \quad (15)$$

The balance equations and conditions

The occurrence of a balanced state in these networks depends on the parameters J_{kl} and $I_k^{(ext)}$, Eq. 14.

With balanced inhibitory and excitatory mean inputs, the network dynamics are dominated by the quenched and temporal fluctuations. The high ($\mathcal{O}(\sqrt{K})$) external and recurrent currents I^{ext} and \bar{I}^{rec} cancel each other at lowest order in K and determine the balanced state firing rate:

$$\mathcal{O}\left(\frac{1}{\sqrt{K}}\right) \approx 0 = I_k^{(ext)} + J_{kE} f_{N_E} \kappa_E \bar{\nu}_E - J_{kI} f_{N_I} \kappa_I \bar{\nu}_I. \quad (16)$$

Self-consistent solutions with two active populations can only be achieved when Eq. 16 holds for both populations and results in:

$$\bar{\nu}_E^{bal} = \bar{\nu}_E = \frac{1}{f_{N_E} \kappa_E} \frac{I_E^{(ext)} J_{II} - I_I^{(ext)} J_{EI}}{J_{EI} J_{IE} - J_{EE} J_{II}} + \mathcal{O}\left(\frac{1}{\sqrt{K}}\right) \quad (17)$$

$$\bar{\nu}_I^{bal} = \bar{\nu}_I = \frac{1}{f_{N_I} \kappa_I} \frac{I_E^{(ext)} J_{IE} - I_I^{(ext)} J_{EE}}{J_{EI} J_{IE} - J_{EE} J_{II}} + \mathcal{O}\left(\frac{1}{\sqrt{K}}\right) \quad (18)$$

In the large network limit ($K \rightarrow \infty$), these balance equations ensure the average input currents \bar{I}_k^0 to remain bounded, while the $\mathcal{O}(K^{-\frac{1}{2}})$ -deviation of the balanced firing rate $\bar{\nu}^{bal}$ is responsible for a small, non-vanishing deviation in finite size networks.

Contrary to the single-population case ($\bar{\nu}^{bal} = \frac{I^{ext}}{J} + \mathcal{O}(\frac{1}{\sqrt{K}})$), the Balanced State in two-population networks can not be obtained for all synaptic weights, as some will lead to exploding ($\bar{\nu}_k \rightarrow \infty$) or quiescent ($\bar{\nu}_k = 0$ Hz) solutions to the firing rate distributions.

External driving currents

The population of excitatory neurons is the only internal source of activity in the network. Even though a state of self-sustained dynamics without an external driving current ($I_E^{ext} = 0$) is possible when inhibitory influence is weak, we will exclude this to focus on models that describe cortical areas driven by afferent, long-range excitatory currents to process and forward information. We therefore require

$$I_E^{ext} > 0. \quad (19)$$

For the inhibitory population, on the other hand, we will allow for a vanishing external drive, thus $I_I^{ext} \geq 0$. This requires the excitatory population to project onto the inhibitory population with non-vanishing synaptic weights $J_{IE} > 0$, to avoid quiescent solutions.

Synaptic weights

Eq. 16 states that the mean input from the inhibitory network not only has to cancel the input from the excitatory neurons, but also the external drive. Thus we

obtain:

$$J_{EE}f_{N_E}\kappa_E\bar{v}_E < J_{EI}f_{N_I}\kappa_I\bar{v}_I, \quad (20)$$

$$J_{IE}f_{N_E}\kappa_E\bar{v}_E \leq J_{II}f_{N_I}\kappa_I\bar{v}_I, \quad (21)$$

where the latter implements the case of a non-driven inhibitory population. Further demanding the inhibitory synapses to have larger influence than the excitatory ones, excludes solutions of exploding excitatory activity from the network dynamics, as the inhibitory feedback can balance the overall excitation for all values:

$$J_{EE}f_{N_E}\kappa_E < J_{EI}f_{N_I}\kappa_I, \quad J_{IE}f_{N_E}\kappa_E < J_{II}f_{N_I}\kappa_I \quad (22)$$

The case of exploding inhibitory activity is excluded by the balanced state dynamics, in which excess inhibition leads to a shutdown of activity and thus prohibits itself.

While quiescent solutions for the inhibitory population are impossible, as long as it receives any input, we exclude quiescent excitatory populations explicitly by demanding

$$\frac{J_{EI}J_{IE}}{J_{EE}J_{II}} > 1, \quad (23)$$

$$I_E^{(ext)}J_{II} > I_I^{(ext)}J_{EI}, \quad I_E^{(ext)}J_{IE} > I_I^{(ext)}J_{EE}, \quad (24)$$

which can be found by solving eq. 17, 18 for $\bar{v}_E = 0$. Summarizing this and eq. 20, 21, 22, we obtain Balanced State networks with constraints:

$$\begin{aligned} \frac{J_{EE}}{J_{EI}} < \frac{J_{IE}}{J_{II}} &\leq \frac{f_{N_I}\kappa_I}{f_{N_E}\kappa_E} \cdot \min \left\{ 1, \frac{\bar{v}_I}{\bar{v}_E} \right\} \quad \text{and} \\ \frac{J_{EE}}{J_{IE}} < \frac{J_{EI}}{J_{II}} &< \frac{I_E^{(ext)}}{I_I^{(ext)}} \end{aligned} \quad (25)$$

To achieve comparable statistics of network dynamics between two-population and one-population models, we can furthermore require the temporal variance of input currents to be equal in both populations (σ_E^2, σ_I^2) and thus conveniently compared to a one-population model ($\sigma_{I(1)}^2$, inhibitory population only), in the case of same firing rates ($\bar{v}_E = \bar{v}_I = \bar{v}_{I(1)}$) and same synaptic time constants ($\tau_{IE} = \tau_{II} = \tau_{I(1)}$):

$$\sigma_E^2 = \sigma_I^2 = \sigma_{I(1)}^2 \quad (26)$$

$$\Leftrightarrow \frac{J_{EE}^2\bar{v}_E}{2\tau_{IE}} + \frac{J_{EI}^2\bar{v}_I}{2\tau_{II}} = \frac{J_{IE}^2\bar{v}_E}{2\tau_{IE}} + \frac{J_{II}^2\bar{v}_I}{2\tau_{II}} = \frac{J_{I(1)}^2\bar{v}_{I(1)}}{2\tau_{I(1)}} \quad (27)$$

$$\Leftrightarrow J_{EE}^2 + J_{EI}^2 = J_{IE}^2 + J_{II}^2 = J^2 \quad (28)$$

We introduce two parameters that reduce the dimensionality of the problem and fulfill the discussed constraints:

$$\begin{aligned} \begin{pmatrix} J_{EE} & J_{EI} \\ J_{IE} & J_{II} \end{pmatrix} &= \begin{pmatrix} \eta\varepsilon & \sqrt{1-(\eta\varepsilon)^2} \\ \varepsilon & \sqrt{1-\varepsilon^2} \end{pmatrix}, \\ \eta < 1, \quad \varepsilon &< \sqrt{\frac{1}{2}} \end{aligned} \quad (29)$$

The excitatory-inhibitory feedback loop strength, ε , defines the impact both populations have on the whole network and the ratio of inter-population excitatory coupling $\eta = \frac{J_{EE}}{J_{IE}}$ describes the difference between the influence of both populations on the excitatory neurons.

C. Neuron model

We utilize the analytically highly tractable Gauss-Rice neuron model [27–29] which follows the dynamics of a leaky integrate-and-fire (LIF) neuron

$$\tau_M \dot{V}(t) = -(V(t) - V_R) + I(t), \quad (30)$$

that generates an AP when the membrane potential $V(t)$ reaches a threshold Ψ_0 from below, but does not include a reset to some baseline potential at spike time. The temporal scale is set by the membrane time constant τ_M . For the sake of readability, the population index k is dropped until it becomes relevant to the calculations.

Without loss of generality, we set $V_R = 0$. Following Jung et al [27] the rate of AP initiation is obtained from counting the number of events at which the potential crosses the threshold value ($V(t) = \Psi_0$) from below ($\dot{V}(t) > 0$):

$$\nu = \langle \delta(V(t) - \Psi_0) \Theta(\dot{V}(t)) \dot{V}(t) \rangle_t. \quad (31)$$

where $\delta(\cdot)$ and $\Theta(\cdot)$ denote the Dirac-Delta-function and Heavyside-function, respectively. Due to ergodicity, the temporal average $\langle \cdot \rangle$ can be expressed by the joint probability density function of the membrane potential and its derivative

$$\nu = \int_{-\infty}^{\infty} \int_{-\infty}^{\infty} dV d\dot{V} P(V, \dot{V}) \delta(V - \Psi_0) \Theta(\dot{V}) \dot{V} \quad (32)$$

Hence, the statistics of V and \dot{V} are sufficient to obtain the firing rate of the neuron model used here.

1. Membrane potential statistics

The joint distribution $P(V, \dot{V})$ - a multidimensional Gaussian, as its variables are driven by a Gaussian distributed input current - is fully characterized by the variables' mean values $\langle V \rangle$, $\langle \dot{V} \rangle$ and the correlation matrix

$$C = \begin{pmatrix} \langle V^2 \rangle & \langle V\dot{V} \rangle \\ \langle V\dot{V} \rangle & \langle \dot{V}^2 \rangle \end{pmatrix} \quad (33)$$

Mean values $\langle V(t) \rangle_t = \langle I(t) \rangle$ and $\langle \dot{V}(t) \rangle_t = 0$ can be extracted directly from Eq. 30 and the constraint of a stationary solution. The assumption of stationarity further

leads to a vanishing cross-correlation, implying independence as they are jointly normal distributed:

$$\begin{aligned}\langle V(t)\dot{V}(t) \rangle &= \left\langle \frac{1}{2} \frac{d}{dt} V^2(t) \right\rangle = \frac{1}{2} \frac{d}{dt} \langle V^2(t) \rangle \\ &= \frac{1}{2} \frac{d}{dt} (\sigma_V^2 + \bar{V}^2) = 0.\end{aligned}$$

where we used the definition of the variance $\sigma_V^2 = \langle V^2(t) \rangle - \langle V(t) \rangle^2$. $P(V, \dot{V})$ (Eq. 32) thus factorizes into the Gaussian pdfs $P(V)$ and $P(\dot{V})$, for which only the respective variances σ_V^2 , $\sigma_{\dot{V}}^2$ are left to obtain for a complete characterization:

Within a neuron, an incoming current pulse $\delta I(t)$ will lead to a temporally extended change in membrane potential according to

$$\delta V(t) = \int_{-\infty}^{+\infty} ds G(t-s) \delta I(s),$$

with $G(\Delta t) = \frac{1}{\tau_M} \exp\left(-\frac{\Delta t}{\tau_M}\right) \Theta(\Delta t)$ the Greens function, obtained from Eq. 30.

The contributions from both populations input currents are additive, $C_{V_k}(\Delta t) = \sum_{l=E,I} C_{V_{kl}}$, allowing to evaluate the integral separately for each population, thus having distinct contributions from each population l . The distinction between input populations l further motivates the reintroduction of the population indices.

Evaluation of the first entry of the correlation matrix Eq. 33 for the contribution of population l results in (see App. A 3 for detailed calculations and the solution in the case $\tau_{I_l} = \tau_M$):

$$C_{V_{kl}}(\Delta t) = \frac{\sigma_{I_l}^2 \tau_{I_l}}{\tau_{I_l}^2 - \tau_M^2} \left[\tau_{I_l} e^{-\frac{|\Delta t|}{\tau_{I_l}}} - \tau_M e^{-\frac{|\Delta t|}{\tau_M}} \right] \quad (34)$$

The variance is obtained from $\sigma_{V_k}^2 = C_{V_k}(0)$, while the variance of the membrane potential derivative is obtained as $\sigma_{\dot{V}_k}^2 = \frac{d^2}{dt^2} C_{V_k}(\Delta t) \Big|_{\Delta t=0}$:

$$\sigma_{V_k}^2 = \sum_{l=E,I} \sigma_{V_{kl}}^2, \quad \sigma_{V_{kl}}^2 = C_{V_{kl}}(0) = \frac{\sigma_{I_l}^2 \tau_{I_l}}{\tau_{I_l} + \tau_M} \quad (35)$$

$$\sigma_{\dot{V}_k}^2 = \sum_{l=E,I} \sigma_{\dot{V}_{kl}}^2, \quad \sigma_{\dot{V}_{kl}}^2 = C_{\dot{V}_{kl}}(0) = \frac{\sigma_{V_{kl}}^2}{\tau_{I_l} \tau_M}. \quad (36)$$

The limiting case $\tau_{I_l} = 0$ would correspond to synapses coupled by δ -pulses that result in a white noise current and a membrane potential following an OU process. In this limit, however, $\sigma_{\dot{V}_k}$ is not finite.

This concludes the derivation of membrane potential pdfs:

$$\begin{aligned}P(V_k, \dot{V}_k) &= P(V_k) P(\dot{V}_k) \\ P(V_k) &= \frac{1}{\sqrt{2\pi\sigma_{V_k}}} \exp\left(-\frac{(V_k - \bar{V}_k)^2}{2\sigma_{V_k}^2}\right) \\ P(\dot{V}_k) &= \frac{1}{\sqrt{2\pi\sigma_{\dot{V}_k}}} \exp\left(-\frac{\dot{V}_k^2}{2\sigma_{\dot{V}_k}^2}\right)\end{aligned}$$

and allows for the evaluation of the input-current dependent firing rate (Eq. 32), using the unitlessness of Eq. 30 to find $\bar{V}_k = \bar{I}_k$, see also [30]:

$$\nu_k(\bar{I}_k^i, \sigma_{V_k}, \sigma_{\dot{V}_k}) = \nu_k^{\max}(\sigma_{V_k}, \sigma_{\dot{V}_k}) \exp\left(-\frac{(\bar{I}_k^i - \Psi_0)^2}{2\sigma_{V_k}^2}\right), \quad (37)$$

$$\nu_k^{\max}(\sigma_{V_k}, \sigma_{\dot{V}_k}) = \frac{1}{2\pi} \frac{\sigma_{\dot{V}_k}}{\sigma_{V_k}}. \quad (38)$$

This is the firing rate transfer function, which translates any Gaussian statistics of input currents to the activity response of a neuron. It takes on a Gaussian shape with maximum firing rate ν^{\max} which has a linear dependence on the ratio of variances $\frac{\sigma_{\dot{V}}}{\sigma_V}$. This simplifies to $(\tau_{I_l} \tau_M)^{-\frac{1}{2}}$ in the case of a single, inhibitory population. In the case of average input currents $\bar{I}_k^i \geq \Psi_0$ the Gauss-Rice model loses plausibility due to the missing reset after threshold crossing. This condition, however, is never met as long as low firing rates are maintained.

D. Mixed receptor types

So far we considered the case of a single synaptic time-constants, but the model remains highly tractable also for a mixture of post-synaptic receptors, Eq. 2. We thus turn to the case of a mixed excitatory post-synaptic kernel, comprised of fast AMPA and slow NMDA receptors. The mixing parameters r_m are associated through $r_{AMPA} = 1 - r_{NMDA}$, henceforth $r_{NMDA} = r$.

The resulting correlation function of the excitatory input current then evaluates to

$$\begin{aligned}C_{I_k}(t) &= J_{kE}^2 \kappa_E \bar{\nu}_E \int_{-\infty}^{\infty} f_E(t-s) f_E(-s) ds \\ &= (1-r)^2 C_A(t) + r^2 C_N(t) \\ &\quad + (1-r)r \frac{J_{kE}^2 \kappa_E \bar{\nu}_E}{\tau_A + \tau_N} \left[\exp\left(-\frac{|t|}{\tau_A}\right) + \exp\left(-\frac{|t|}{\tau_N}\right) \right],\end{aligned}$$

where $C_A(t)$ denotes the excitatory correlation function obtained from a network of neurons with only AMPA-receptors and $C_N(t)$ is the excitatory correlation function of a network of neurons with only NMDA-receptors, Eq. 10. The correlation function of the membrane potential from the excitatory input again can be calculated according to Appendix A 3:

$$C_{V_{kE}}(t) = \int_{-\infty}^{\infty} C_{I_k}(s) G^{(2)}(s-t) ds = \frac{J_{kE}^2 \kappa_E \bar{\nu}_E}{\tau_A^2 - \tau_M^2} \left[\frac{(1-r)^2}{2} + \frac{(1-r)r\tau_A}{\tau_A + \tau_N} \right] \left[\tau_A \exp\left(-\frac{|t|}{\tau_A}\right) - \tau_M \exp\left(-\frac{|t|}{\tau_M}\right) \right] \\ + \frac{J_{kE}^2 \kappa_E \bar{\nu}_E}{\tau_N^2 - \tau_M^2} \left[\frac{r^2}{2} + \frac{(1-r)r\tau_N}{\tau_A + \tau_N} \right] \left[\tau_N \exp\left(-\frac{|t|}{\tau_N}\right) - \tau_M \exp\left(-\frac{|t|}{\tau_M}\right) \right].$$

The variance follows as

$$\sigma_{V_{kE}}^2 = C_{V_k}(0) = \overbrace{\frac{J_{kE}^2 \kappa_E \bar{\nu}_E}{\tau_A + \tau_M} \left[\frac{(1-r)^2}{2} + \frac{(1-r)r\tau_A}{\tau_A + \tau_N} \right]}^{=: \sigma_{V,A}^2} + \underbrace{\frac{J_{kE}^2 \kappa_E \bar{\nu}_E}{\tau_N + \tau_M} \left[\frac{r^2}{2} + \frac{(1-r)r\tau_N}{\tau_A + \tau_N} \right]}_{=: \sigma_{V,N}^2}. \quad (39)$$

We obtain the variance of the derivative of the membrane potential, originating from excitatory sources as:

$$\sigma_{V_{kE}}^2 = \frac{\partial^2 C_{V_k}(0)}{\partial t^2} \quad (40) \\ = -\frac{1}{\tau_A \tau_M} \frac{J_{kE}^2 \kappa_E \bar{\nu}_E}{(\tau_A + \tau_M)} \left[\frac{(1-r)^2}{2} + \frac{(1-r)r\tau_A}{\tau_A + \tau_N} \right] \\ - \frac{1}{\tau_N \tau_M} \frac{J_{kE}^2 \kappa_E \bar{\nu}_E}{(\tau_N + \tau_M)} \left[\frac{r^2}{2} + \frac{(1-r)r\tau_N}{\tau_A + \tau_N} \right] \\ = -\frac{\sigma_{V,A}^2}{\tau_A \tau_M} - \frac{\sigma_{V,N}^2}{\tau_N \tau_M}. \quad (41)$$

E. Introducing network heterogeneity

Following [11, 12], we include a heterogeneity $\alpha_{0,k}$ in the firing threshold of population k :

$$\Psi_{0,k} \rightarrow \Psi_0 + \alpha_{0,k} \cdot x$$

where x is a Gaussian random number with mean 0 and unit variance. Note that, in a linear neuron model such as ours, a higher firing threshold of a neuron is equivalent to a lower received average input current, as both result in an additional depolarization required for emitting an action potential. Therefore the total quenched variance including Gaussian threshold differences between individual neurons and contributions from the random connectivity is defined as:

$$\alpha_k^2 := \alpha_{I_k}^2 + \alpha_{0,k}^2, \quad q_k \rightarrow q_k + q_{0,k},$$

where $q_{0,k} = \alpha_{0,k}^2 / J_{kl}^2$.

F. Firing rate distributions

The distribution of average input currents $\rho(I)$ (Eq. 15) together with the firing rate response of a neuron to a mean input current $\nu(I)$ (Eq. 38) allows for

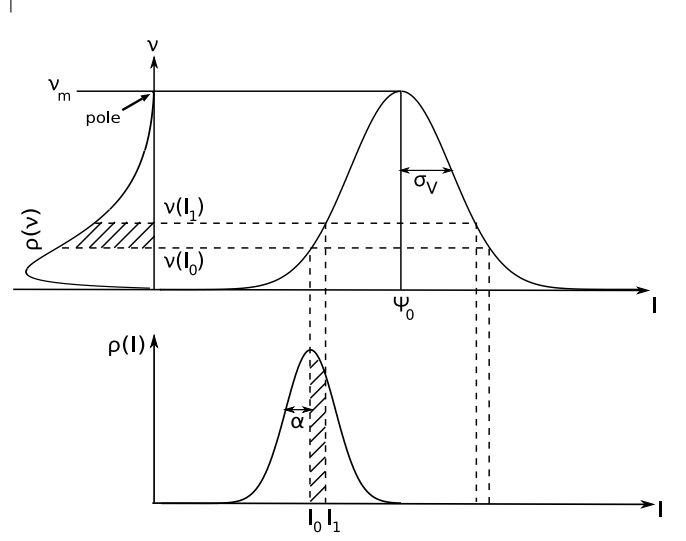


FIG. 3. The firing rate distribution is obtained by a transformation from the distribution of mean input currents $\rho(I)$ (lower graph) through the transfer function of the Gauss-Rice neuron $\nu(I)$ (upper right graph); left: resulting firing rate $\rho(\nu)$. Dashed lines sketch, how probability mass is conserved under the transformation. Once the two former distributions are known the firing rate distribution can be determined. $\nu_m = \bar{\nu}^{\max}$.

the calculation of the distribution of average firing rates across each population k (population index dropped), using a transformation of probability density functions (see Fig. 3) as:

$$\rho(\nu) = \rho(I_-(\nu)) \left| \frac{dI_-}{d\nu} \right| + \rho(I_+(\nu)) \left| \frac{dI_+}{d\nu} \right|, \quad (42)$$

where $-$ and $+$ are the indices to the rising and falling (non-realistic) part of the transfer function, respectively. The inverse of Eq. 38 gives I and its absolute derivative for both parts of the transfer function:

$$\bar{I}_{\pm}(\nu) = \Psi_0 \pm \sigma_V \sqrt{-2 \ln \frac{\nu}{\nu^{\max}}} \\ \left| \frac{dI_{\pm}}{d\nu} \right| = \frac{\sigma_V}{\nu \sqrt{-2 \ln \frac{\nu}{\nu^{\max}}}}$$

Evaluating Eq. 42 and using $\exp(x) + \exp(-x) \equiv 2 \cosh(x)$, the analytical form of the firing rate distribution

bution is:

$$\rho(\nu) = \frac{\gamma}{\nu^{\max} \sqrt{-\pi \ln \frac{\nu}{\nu^{\max}}}} \exp\left(-\frac{\delta^2}{2}\right) \left(\frac{\nu}{\nu^{\max}}\right)^{(\gamma^2-1)} \cosh\left(\gamma\delta\sqrt{-2\ln\frac{\nu}{\nu^{\max}}}\right) \quad (43)$$

with $\gamma^2 := \frac{\sigma_V^2}{\alpha^2}$, $\delta := \frac{\Psi_0 - \bar{I}_0}{\alpha}$.

The log firing rate-distribution can be used for further analysis of extrema and evaluates to

$$\begin{aligned} \ln \rho(\nu) &= -\ln\left(\frac{\nu^{\max}}{\gamma} \sqrt{-\pi \ln \frac{\nu}{\nu^{\max}}}\right) - \frac{\delta^2}{2} + \\ &\quad (\gamma^2 - 1) \ln \frac{\nu}{\nu^{\max}} + \ln\left(\cosh \gamma\delta\sqrt{-2\ln\frac{\nu}{\nu^{\max}}}\right) \\ &\approx \sqrt{-\ln \frac{\nu}{\nu^{\max}}} \left(\gamma\delta\sqrt{2} - (\gamma^2 - 1) \sqrt{-\ln \frac{\nu}{\nu^{\max}}}\right) \end{aligned} \quad (44)$$

where the approximation on the last line holds in the low firing rate limit $\nu \rightarrow 0^+$. It follows from rewriting $2 \cosh(\xi) = \exp(\xi) + \exp(-\xi) \approx \exp(\xi)$ and identifies the dominant term $\xi = \gamma\delta\sqrt{-2\ln\frac{\nu}{\nu^{\max}}}$, as $\lim_{x \rightarrow 0} \ln(x) \rightarrow -\infty$.

Peaked distributions

The exact logarithmic distribution can further be used to obtain the firing rate peak position by finding ν at which $\frac{d}{d\nu} \ln \rho(\nu) = 0$, $\frac{d^2}{d\nu^2} \ln \rho(\nu) < 0$, resulting in

$$\nu^{(p)} = \nu^{\max} e^{-\frac{\gamma^2 \delta^2 - 2(\gamma^2 - 1) + \gamma\delta\sqrt{\gamma^2 \delta^2 - 4(\gamma^2 - 1)}}{4(\gamma^2 - 1)^2}} \quad (45)$$

$$\Rightarrow 4(\gamma^2 - 1) < \gamma^2 \delta^2, \quad (46)$$

with Eq. 46 defining the requirement for a peaked distribution to occur at all. If it is violated, the firing rate distribution monotonously rises from $\rho(\nu = 0) = 0$ towards $\rho(\nu = \nu^{\max}) \rightarrow \infty$. Equality of the terms defines the firing rate $\nu_{\text{no peak}}$, at which a transition between peaked and non-peaked distributions occurs.

To measure the skewness of the distribution, we define the *skewness coefficient* χ as the log-ratio of peak position $\nu^{(p)}$ to mean firing rate $\bar{\nu}$:

$$\chi = -\log_{10} \frac{\nu^{(p)}}{\bar{\nu}} \quad (47)$$

Different values of χ describe, how strongly the distribution leans to one side. A positive value corresponds to right-skewed firing rate distributions, where the majority of the probability mass accumulates at firing rates lower than the average. For $\chi = 0$ the peak coincides with the mean rate, for $\chi = 1$ the peak occurs at one tenth of the mean, etc.

III. RESULTS

In this work, we present a model of a neuronal network for which we derive an analytically solvable solution to the firing rate distribution (Methods II). The model is able to implement firing threshold heterogeneities, can describe two interconnected neuronal populations, with the ability to add more and includes the possibility for population-specific mixed post-synaptic receptor types.

We use the analytically tractable Gauss-Rice neuron model in a balanced state network to describe distributions of recurrent input currents and according membrane potentials, from which we derive the firing rate distribution for population k :

$$\rho(\nu_k^i) = \frac{\gamma_k}{\nu_k^{\max} \sqrt{-\pi \ln \frac{\nu_k^i}{\nu_k^{\max}}}} \exp\left(-\frac{\delta_k^2}{2}\right) \left(\frac{\nu_k^i}{\nu_k^{\max}}\right)^{\gamma_k^2-1} \cosh\left(\gamma_k \delta_k \sqrt{-2\ln\frac{\nu_k^i}{\nu_k^{\max}}}\right), \text{ with } \delta_k := \frac{\Psi_0 - \bar{I}_k}{\alpha_k}, \quad \gamma_k := \frac{\sigma_{V_k}}{\alpha_k} \quad (48)$$

with the *dark matter exponent* γ , the ratio of temporal variance of membrane potential fluctuation σ_V^2 and the quenched variance of input currents across the network α^2 and the relative distance δ of mean input current I_0 to the firing threshold Ψ_0 .

A. Selfconsistent solutions to the firing rate distribution

Eq. 48 depends on both, the first moment (directly via $\bar{\nu}_l := [\nu_l^i]_i$, indirectly via the temporal variance $\sigma_{V_l}^2$, Eq. 36) and the second moment (with $\alpha_{kl}^2 = J_{kl}^2 f_{N_l} \kappa_l q_l$; $q_l := [(\nu_l^i)^2]_i$, Eq. 9) of the firing rates ν_l . These moments can be calculated population-wise from the distribution of input currents, Eq. 15 and the firing rate

response Eq. 38:

$$\left[\nu_k^{\{m\}} \right] = \int Dx \left[\nu_k^{\max} \exp \left(-\frac{(\bar{I}_k^0 + \alpha_k x - \Psi_0)^2}{2\sigma_{V_k}^2} \right) \right]^m,$$

where the average input current to each neuron $\bar{I}_k^0 + \alpha_k x$ is drawn from a 0-centered Gaussian distribution of x with unit variance: $Dx = dx(2\pi)^{-\frac{1}{2}} \exp(-x^2/2)$. Solving the integral for $m = 1$ and $m = 2$, we obtain

$$\bar{\nu}_k = \nu_k^{\max} \frac{\sigma_{V_k}}{\sqrt{\alpha_k^2 + \sigma_{V_k}^2}} \exp \left(-\frac{(\bar{I}_k^0 - \Psi_0)^2}{2(\alpha_k^2 + \sigma_{V_k}^2)} \right) \quad (49)$$

$$q_k = (\nu_k^{\max})^2 \frac{\sigma_{V_k}}{\sqrt{2\alpha_k^2 + \sigma_{V_k}^2}} \exp \left(-\frac{(\bar{I}_k^0 - \Psi_0)^2}{2\alpha_k^2 + \sigma_{V_k}^2} \right) \quad (50)$$

Standard deviations σ_{V_k} , α_k , mean input current \bar{I}_k^0 and maximum firing rate ν_k^{\max} contain contributions from both populations, thus forming a transcendental equation, relating first and second moments of ν_l to one another and thus defining a path towards a self-consistent solution to the model:

Solving Eq. 49, 50 for $(\bar{I}_k^0 - \Psi_0)^2$ both imposes a constraint on the parameter range in which self-consistent values can be found ($\bar{\nu}^*, q^*$) can be found (requiring real-valued input currents $I^2 \geq 0$) and defines the a relation to calculate them:

$$\begin{aligned} I_k^2 &= (\bar{I}_k^0 - \Psi_0)^2 \\ &= \overbrace{\left(\alpha_k^2 + \sigma_{V_k}^2 \right) \ln \left[\left(\frac{\bar{\nu}_k^*}{\nu_k^{\max}} \right)^2 \left(\frac{\alpha_k^2}{\sigma_{V_k}^2} + 1 \right) \right]}^{=: \bar{I}_{\bar{\nu}}(\bar{\nu}, q)} \\ &= \underbrace{\left(\alpha_k^2 + \frac{1}{2}\sigma_{V_k}^2 \right) \ln \left[\left(\frac{q_k^*}{(\nu_k^{\max})^2} \right)^2 \left(2\frac{\alpha_k^2}{\sigma_{V_k}^2} + 1 \right) \right]}_{=: \bar{I}_q(\bar{\nu}, q)} \end{aligned} \quad (51)$$

It is a transcendent equation that can be solved numerically exact (e.g. by a root-finding algorithm) or - in the one-population case - analytically by an approximation presented below, allowing us for the first time to present a closed form solution of the firing rate distribution in a balanced state network.

1. Analytical solution of the firing rate distribution

Self-consistent values $(\bar{\nu}_k^*, q_k^*)$ are obtained by finding the intersection of the solutions for the input current $\bar{I}_k^0 - \Psi_0$ from the evaluation of the first and second moment, Eq. 51, respectively. In the case of a network composed of a single population only (thus, dropping population indices), we notice the small slope of the former,

Eq. 49, allowing us to approximate its solution by a constant value. Using $q = \bar{\nu}^2$ we obtain an approximate value $\bar{I}_{\bar{\nu}}^2(\bar{\nu}, \bar{\nu}^2)$, not much different from the exact solution $\bar{I}_{\bar{\nu}}^2(\bar{\nu}^*, q^*)$. Inserting this and the approximation of the quenched variance $\alpha_k^2 \approx J^2 f_{\mathcal{N}} \bar{\nu}^2$ (dropping κ , as it merely describes the relative sizes of different populations) into equation 50 gives an analytically solvable expression for the second moment:

$$q = \frac{1}{\sqrt{1 + 2\tau_q \left(\bar{\nu} + \frac{q_0}{\bar{\nu}} \right)}} \left(1 + \tau_q \left(\bar{\nu} + \frac{q_0}{\bar{\nu}} \right) \right)^{1-\epsilon} \nu_{\max}^{2\epsilon} \bar{\nu}^{2-2\epsilon} \quad (52)$$

$$\text{with } \epsilon = \frac{\tau_q (\bar{\nu}^2 + q_0)}{\bar{\nu} + 2\tau_q (\bar{\nu}^2 + q_0)}, \quad \tau_q = 2(\tau_I + \tau_M)$$

The closed form solution allows for a discussion of marginal cases, specifically in the low firing rate regime $\bar{\nu} \rightarrow 0$: A homogeneous network ($\alpha_0^2 = \frac{q_0}{J} = 0$) gives the initial approximation of a quadratic dependence $q \approx \bar{\nu}^2$. However, as soon as an arbitrary amount of inhomogeneity $q_0 \geq 0$ is added, the second moment initially grows linear with the firing rate $q \approx \frac{\nu_{\max}}{\sqrt{2}} \bar{\nu}$. Finally, Eq. 52 allows us, for the first time to our knowledge, to write down a closed form solution of a firing rate distribution of a neural network.

IV. DISCUSSION

We presented an analytically tractable model of balanced state networks of spiking neurons in local cortical circuits. We derived closed-form equations for the firing rate distributions in one and two population networks. Neurons may be connected by synapses mediating arbitrary mixtures of slow and fast currents. In the large system limit, the shape and range of the firing rate distribution is determined by self-consistency equations for a small number of order parameters of population heterogeneity. We find that biological properties of neurons and synapses impact the emergent firing rate heterogeneity through a set of effective parameters that determine the firing rate distribution. In our model, firing rate distributions are not mathematically log-normal but can easily reproduce the form and range of skewed rate distributions observed frequently in experiments [1–10]. Besides log-normal-like firing rate distributions, the model can also reproduce the monotonically decreasing rate distribution originally reported for the binary neuron model of the balanced state [11, 12]. Our model should thus also enable to systematically examine the range of biological parameters consistent with realistic rate distributions and potentially predict conditions under which the generic form of rate heterogeneity breaks down.

These advancements are based on several properties of the Gauss-Rice neuron model. Firstly, the Gauss-Rice model permits the derivation of closed-form solutions for properties such as the noisy f-I-curve or the population

rate dynamic responses for arbitrary temporal correlations in the synaptic input currents with correlation functions differentiable at zero lag time [30–35]. In the current study, we used this advantage to examine networks in which cortical excitatory synapses exhibit a mix of fast and slow currents such that voltage fluctuations exhibit multiple timescales. This is necessary to realistically model circuits in which excitatory synapses contain both AMPA and NMDA receptors, a feature of essentially every cortical network. In principle, classical LIF networks could be treated in a formally analogous fashion [36] but only with excessive formal effort and much lower tractability. Secondly, the Gauss-Rice model with current-based synapses exhibits a Gaussian shaped noisy f-I-curve [30–35]. This feature enabled us to directly calculate the population and disorder averages in the self-consistency equations for the firing rate heterogeneity. For biological plausibility of the solutions of these self-

consistency equations, only the rising part of f-I-curve should be effectively used. This condition is guaranteed in low-rate settings and can be easily validated in general.

Due to its great tractability, we expect that the type of circuit models introduced here will enable to advance a suite of questions and problems in modelling cortical circuits that previously were out of reach for analytical study. These include the treatment of emergent response function and tuning curve heterogeneity in sensory cortical networks, analytical heterogeneity of working memory circuits, the analysis of spatially extended, multilayer and multi-area circuits and potentially the dynamics of rate distributions in dynamic network states. For all these problems, our approach paves the way to systematically and efficiently examine the impact of quantitative cellular parameters such as membrane and synaptic time constants, AMPA to NMDA receptor ratio or cell-to-cell heterogeneity in excitability.

-
- [1] H. Hirase, X. Leinekugel, A. Czurkó, J. Csicsvari, and G. Buzsáki, “Firing rates of hippocampal neurons are preserved during subsequent sleep episodes and modified by novel awake experience,” *Proceedings of the National Academy of Sciences*, vol. 98, no. 16, pp. 9386–9390, Jul. 2001, publisher: Proceedings of the National Academy of Sciences. [Online]. Available: <https://www.pnas.org/doi/10.1073/pnas.161274398>
 - [2] F. P. Battaglia, G. R. Sutherland, S. L. Cowen, B. L. McNaughton, and K. D. Harris, “Firing rate modulation: a simple statistical view of memory trace reactivation,” *Neural Networks: The Official Journal of the International Neural Network Society*, vol. 18, no. 9, pp. 1280–1291, Nov. 2005.
 - [3] M. Shafi, Y. Zhou, J. Quintana, C. Chow, J. Fuster, and M. Bodner, “Variability in neuronal activity in primate cortex during working memory tasks,” *Neuroscience*, vol. 146, no. 3, pp. 1082–1108, May 2007.
 - [4] T. Hromádka, M. R. DeWeese, and A. M. Zador, “Sparse Representation of Sounds in the Unanesthetized Auditory Cortex,” *PLOS Biology*, vol. 6, no. 1, p. e16, Jan. 2008, publisher: Public Library of Science. [Online]. Available: <https://journals.plos.org/plosbiology/article?id=10.1371/journal.pbio.0060016>
 - [5] D. H. O’Connor, S. P. Peron, D. Huber, and K. Svoboda, “Neural activity in barrel cortex underlying vibrissa-based object localization in mice,” *Neuron*, vol. 67, no. 6, pp. 1048–1061, Sep. 2010.
 - [6] A. Peyrache, N. Dehghani, E. N. Eskandar, J. R. Madsen, W. S. Anderson, J. A. Donoghue, L. R. Hochberg, E. Halgren, S. S. Cash, and A. Destexhe, “Spatiotemporal dynamics of neocortical excitation and inhibition during human sleep,” *Proceedings of the National Academy of Sciences of the United States of America*, vol. 109, no. 5, pp. 1731–1736, Jan. 2012.
 - [7] K. Mizuseki and G. Buzsáki, “Preconfigured, skewed distribution of firing rates in the hippocampus and entorhinal cortex,” *Cell Reports*, vol. 4, no. 5, pp. 1010–1021, Sep. 2013.
 - [8] M. A. Busche, C. Grienberger, A. D. Keskin, B. Song, U. Neumann, M. Staufenbiel, and A. Konnerth, “Decreased amyloid- β and increased neuronal hyperactivity by immunotherapy in Alzheimer’s models,” *Nature neuroscience*, vol. 18, no. 12, pp. 1725–1728, 2015.
 - [9] S. Shoham, D. H. O’Connor, and R. Segev, “How silent is the brain: is there a “dark matter” problem in neuroscience?” *Journal of Comparative Physiology A*, vol. 192, no. 8, pp. 777–784, Aug. 2006. [Online]. Available: <https://doi.org/10.1007/s00359-006-0117-6>
 - [10] G. Buzsáki and K. Mizuseki, “The log-dynamic brain: how skewed distributions affect network operations,” *Nature Reviews Neuroscience*, vol. 15, no. 4, pp. 264–278, Apr. 2014, number: 4 Publisher: Nature Publishing Group. [Online]. Available: <https://www.nature.com/articles/nrn3687>
 - [11] C. van Vreeswijk and H. Sompolinsky, “Chaos in Neuronal Networks with Balanced Excitatory and Inhibitory Activity,” *Science*, vol. 274, no. 5293, pp. 1724–1726, Dec. 1996, publisher: American Association for the Advancement of Science. [Online]. Available: <https://www.science.org/doi/10.1126/science.274.5293.1724>
 - [12] —, “Chaotic balanced state in a model of cortical circuits,” *Neural Computation*, vol. 10, no. 6, pp. 1321–1371, Aug. 1998.
 - [13] A. Roxin, N. Brunel, D. Hansel, G. Mongillo, and C. v. Vreeswijk, “On the Distribution of Firing Rates in Networks of Cortical Neurons,” *Journal of Neuroscience*, vol. 31, no. 45, pp. 16 217–16 226, Nov. 2011, publisher: Society for Neuroscience Section: Articles. [Online]. Available: <https://www.jneurosci.org/content/31/45/16217>
 - [14] M. Monteforte and F. Wolf, “Dynamical Entropy Production in Spiking Neuron Networks in the Balanced State,” *Physical Review Letters*, vol. 105, no. 26, p. 268104, Dec. 2010, publisher: American Physical Society. [Online]. Available: <https://link.aps.org/doi/10.1103/PhysRevLett.105.268104>
 - [15] —, “Dynamic Flux Tubes Form Reservoirs of Stability in Neuronal Circuits,” *Physical Review X*, vol. 2, no. 4, p. 041007, Nov. 2012, publisher:

- American Physical Society. [Online]. Available: <https://link.aps.org/doi/10.1103/PhysRevX.2.041007>
- [16] A. Renart, J. de la Rocha, P. Bartho, L. Hollender, N. Parga, A. Reyes, and K. D. Harris, "The Asynchronous State in Cortical Circuits," *Science*, vol. 327, no. 5965, pp. 587–590, Jan. 2010, publisher: American Association for the Advancement of Science. [Online]. Available: <https://www.science.org/doi/10.1126/science.1179850>
 - [17] D. J. Amit and N. Brunel, "Dynamics of a recurrent network of spiking neurons before and following learning," *Network: Computation in Neural Systems*, vol. 8, no. 4, pp. 373–404, Jan. 1997, publisher: Taylor & Francis eprint: <https://doi.org/10.1088/0954-898X.8.4.003>. [Online]. Available: <https://doi.org/10.1088/0954-898X.8.4.003>
 - [18] N. Brunel, "Dynamics of Sparsely Connected Networks of Excitatory and Inhibitory Spiking Neurons," *Journal of Computational Neuroscience*, vol. 8, no. 3, pp. 183–208, May 2000. [Online]. Available: <https://doi.org/10.1023/A:1008925309027>
 - [19] W. R. Softky and C. Koch, "The highly irregular firing of cortical cells is inconsistent with temporal integration of random EPSPs," *The Official Journal of the Society for Neuroscience*, vol. 13, no. 1, pp. 334–350, Jan. 1993.
 - [20] T. S. Otis and I. Mody, "Modulation of decay kinetics and frequency of GABAA receptor-mediated spontaneous inhibitory postsynaptic currents in hippocampal neurons," *Neuroscience*, vol. 49, no. 1, pp. 13–32, Jul. 1992.
 - [21] E. Sigel and M. E. Steinmann, "Structure, Function, and Modulation of GABAA Receptors *," *Journal of Biological Chemistry*, vol. 287, no. 48, pp. 40 224–40 231, Nov. 2012, publisher: Elsevier. [Online]. Available: [https://www.jbc.org/article/S0021-9258\(20\)62166-4/abstract](https://www.jbc.org/article/S0021-9258(20)62166-4/abstract)
 - [22] D. Attwell and A. Gibb, "Neuroenergetics and the kinetic design of excitatory synapses," *Nature Reviews Neuroscience*, vol. 6, no. 11, pp. 841–849, Nov. 2005, number: 11 Publisher: Nature Publishing Group. [Online]. Available: <https://www.nature.com/articles/nrn1784>
 - [23] S. F. Traynelis, L. P. Wollmuth, C. J. McBain, F. S. Menenti, K. M. Vance, K. K. Ogden, K. B. Hansen, H. Yuan, S. J. Myers, and R. Dingledine, "Glutamate receptor ion channels: structure, regulation, and function," *Pharmacological Reviews*, vol. 62, no. 3, pp. 405–496, Sep. 2010.
 - [24] A. Compte, C. Constantinidis, J. Tegnér, S. Raghavachari, M. V. Chafee, P. S. Goldman-Rakic, and X.-J. Wang, "Temporally Irregular Mnemonic Persistent Activity in Prefrontal Neurons of Monkeys During a Delayed Response Task," *Journal of Neurophysiology*, vol. 90, no. 5, pp. 3441–3454, Nov. 2003, publisher: American Physiological Society. [Online]. Available: <https://journals.physiology.org/doi/full/10.1152/jn.00949.2002>
 - [25] J. N. D. Kerr, D. Greenberg, and F. Helmchen, "Imaging input and output of neocortical networks in vivo," *Proceedings of the National Academy of Sciences*, vol. 102, no. 39, pp. 14 063–14 068, Sep. 2005, publisher: Proceedings of the National Academy of Sciences. [Online]. Available: <https://www.pnas.org/doi/10.1073/pnas.0506029102>
 - [26] P. Dayan and L. F. Abbott, *Theoretical neuroscience: computational and mathematical modeling of neural systems*, ser. Computational neuroscience. Cambridge, Mass: Massachusetts Institute of Technology Press, 2001.
 - [27] P. Jung, "Stochastic resonance and optimal design of threshold detectors," *Physics Letters A*, vol. 207, no. 1, pp. 93–104, Oct. 1995. [Online]. Available: <https://www.sciencedirect.com/science/article/pii/037596019500636H>
 - [28] B. Naundorf, F. Wolf, and M. Volgushev, "Unique features of action potential initiation in cortical neurons," *Nature*, vol. 440, no. 7087, pp. 1060–1063, Apr. 2006.
 - [29] S. O. Rice, "Mathematical analysis of random noise," *The Bell System Technical Journal*, vol. 23, no. 3, pp. 282–332, Jul. 1944, conference Name: The Bell System Technical Journal.
 - [30] T. Tchumatchenko, T. Geisel, M. Volgushev, and F. Wolf, "Signatures of Synchrony in Pairwise Count Correlations," *Frontiers in Computational Neuroscience*, vol. 4, p. 1, Apr. 2010. [Online]. Available: <https://www.ncbi.nlm.nih.gov/pmc/articles/PMC2857958/>
 - [31] T. Tchumatchenko, A. Malyshev, T. Geisel, M. Volgushev, and F. Wolf, "Correlations and Synchrony in Threshold Neuron Models," *Physical Review Letters*, vol. 104, no. 5, p. 058102, Feb. 2010, publisher: American Physical Society. [Online]. Available: <https://link.aps.org/doi/10.1103/PhysRevLett.104.058102>
 - [32] T. Tchumatchenko and F. Wolf, "Representation of Dynamical Stimuli in Populations of Threshold Neurons," *PLOS Computational Biology*, vol. 7, no. 10, p. e1002239, Oct. 2011, publisher: Public Library of Science. [Online]. Available: <https://journals.plos.org/ploscompbiol/article?id=10.1371/journal.pcbi.1002239>
 - [33] T. Tchumatchenko, T. Geisel, M. Volgushev, and F. Wolf, "Spike Correlations – What Can They Tell About Synchrony?" *Frontiers in Neuroscience*, vol. 5, 2011. [Online]. Available: <https://www.frontiersin.org/articles/10.3389/fnins.2011.00068>
 - [34] E. Di Bernardino, J. León, and T. Tchumatchenko, "Cross-Correlations and Joint Gaussianity in Multivariate Level Crossing Models," *The Journal of Mathematical Neuroscience*, vol. 4, no. 1, p. 22, Apr. 2014. [Online]. Available: <https://doi.org/10.1186/2190-8567-4-22>
 - [35] M. P. Touzel and F. Wolf, "Complete Firing-Rate Response of Neurons with Complex Intrinsic Dynamics," *PLOS Computational Biology*, vol. 11, no. 12, p. e1004636, Dec. 2015, publisher: Public Library of Science. [Online]. Available: <https://journals.plos.org/ploscompbiol/article?id=10.1371/journal.pcbi.1004636>
 - [36] R. Moreno-Bote and N. Parga, "Response of integrate-and-fire neurons to noisy inputs filtered by synapses with arbitrary timescales: firing rate and correlations," *Neural Computation*, vol. 22, no. 6, pp. 1528–1572, Jun. 2010.

Appendix A: Appendices

1. Variance of the compound spike train

Due to independence of the connectivity matrix A_{kl}^{ij} , the solutions to the compound spike train variance for different populations decouple and can be obtained as a superposition of the solutions to the distinct populations.

The second moment for one population yields:

$$\begin{aligned} [\Omega_i^2]_i &= \left[\left(\sum_{j=1}^N A_{ij} \nu_j \right) \left(\sum_{k=1}^N A_{ik} \nu_k \right) \right]_i \\ &= \sum_{j=1}^N \sum_{k=1}^N [A_{ij} A_{ik}]_i \nu_j \nu_k \end{aligned}$$

This can be split into a diagonal ($j = k$) and an off-diagonal ($j \neq k$) term:

$$\begin{aligned} [\Omega_i^2]_i &= \sum_{j=1}^N [A_{ij}]_i \nu_j^2 + \sum_{j=1}^N \sum_{k \neq j}^N [A_{ij}]_i [A_{ik}]_i \nu_j \nu_k \\ &= K [\nu_j^2]_j + \sum_{j=1}^N [A_{ij}]_i \nu_j \sum_{k=1}^N [A_{ik}]_i \nu_k - \sum_{j=1}^N [A_{ij}]_i^2 \nu_j^2 \\ &= K [\nu_j^2]_j + K^2 \bar{\nu}^2 - \frac{1}{N} [(K_j^{\text{out}})^2]_j [\nu_j]_j^2 \end{aligned}$$

As the out-degree follows a poisson distribution, the second moment is $K^2 + K$, which vanishes against N and

the variance is obtained as:

$$\text{Var}(\Omega) = [\Omega_i^2]_i - [\Omega_i]_i^2 = K [\nu_j^2]_j + K^2 \bar{\nu}^2 - K^2 \bar{\nu}^2 = Kq,$$

where q denotes the second moment of the firing rate distribution. The solution to multiple populations l is obtained by substituting $K \rightarrow \kappa_l K$ for each population, resulting in:

$$\text{Var}(\Omega) = K \sum_l \kappa_l q_l.$$

2. Input current

a. Averaged input current

Similar to App. A 1, we can obtain the average input current to neuron i as the sum of average input currents from either population, following from the statistics of the compound spike train, Eq. 4.

The probability of a specific spike train realization from a single population is

$$P(\{t^{(p)}\} | \Omega(t)) = \frac{e^{-\int_0^T dt \Omega(t)}}{N_{\text{AP}}!} \prod_{p=1}^{N_{\text{AP}}} \Omega(t^{(p)}),$$

with the factor $1/N_{\text{AP}}!$ accounting for the unordered nature of such randomized sequences. As the PSCs are assumed to be uncorrelated, the integration over spike times $t^{(p)}$ is interchangeable. The average current within time interval $t \in [0, T]$ is

$$\begin{aligned} \langle I_i(t) \rangle &= \sum_{N_{\text{AP}}=0}^{\infty} \int_0^T \cdots \int_0^T \left(\prod_{p=1}^{N_{\text{AP}}} dt^{(p)} \right) I(t, \{t^{(p)}\}) P(\{t^{(p)}\} | \Omega_i(t^{(p)}\}) \\ &= \sum_{N_{\text{AP}}=0}^{\infty} \int_0^T \cdots \int_0^T \left(\prod_{p=1}^{N_{\text{AP}}} dt^{(p)} \right) \left(J \sum_{p'=1}^{N_{\text{AP}}} f(t - t^{(p')}) \right) \frac{e^{-\int_0^T ds \Omega_i(s)}}{N_{\text{AP}}!} \prod_{p''=1}^{N_{\text{AP}}} \Omega_i(t^{(p'')}) \\ &= J e^{-\int_0^T ds \Omega_i(s)} \sum_{N_{\text{AP}}=1}^{\infty} \frac{1}{(N_{\text{AP}} - 1)!} \left(\int_0^T ds \Omega_i(s) \right)^{N_{\text{AP}}-1} \int_0^T dt^{(1)} f(t - t^{(1)}) \Omega_i(t^{(1)}), \end{aligned}$$

where $\langle \cdot \rangle$ denotes time average. The last line uses that all N_{AP} integrals over one PSC yield the same result, as long as the kernel $f(t - t^{(p)})$ is within the interval $t \in [0, T]$. As the PSCs are equal, we can chose $t^{(1)}$ to be representative of all N_{AP} events. The sum - neglecting the first, vanishing term of $N_{\text{AP}} = 0$ - is the definition of the exponential series, canceling with the previous term

and the equation then reads

$$\langle I_i(t) \rangle = \frac{J}{\sqrt{K}} \int_0^T dt^{(1)} f(t - t^{(1)}) \Omega_i(t^{(1)}) = \frac{J}{\sqrt{K}} f_{\mathcal{N}} \Omega_i, \quad (\text{A1})$$

where the last equation holds in the stationary case ($\Omega_i(t^{(1)}) = \Omega_i$), with the $f_{\mathcal{N}}$ the integral over the kernel.

b. Input current covariance

The statistics of input current temporal fluctuations can be captured by the input current covariance function:

$$\begin{aligned} C_{I_i}(t, t') &:= \langle \delta I^i(t) \delta I^i(t') \rangle \\ &= 2 \underbrace{\langle \delta I_E^i(t) \delta I_I^i(t') \rangle}_{\text{uncorrelated} \rightarrow 0} + \sum_{l=E, I} \langle \delta I_l^i(t) \delta I_l^i(t') \rangle. \end{aligned}$$

We can thus evaluate the covariance for each population separately (dropping population indices):

$$\begin{aligned} C_{I_i}(t, t') &:= \langle \delta I_i(t) \delta I_i(t') \rangle \\ &= \langle I_i(t) I_i(t') \rangle - \langle I_i(t) \rangle \langle I_i(t') \rangle \end{aligned} \quad (\text{A2})$$

Here $\delta I_i(t)$ is the deviation of $I_i(t)$ from the time average $\langle I_i(t) \rangle$. The second term is already known from Eq. 7 and

the first one can be obtained as:

$$\begin{aligned} \langle I(t) I(t') \rangle &= \left\langle J \sum_{p'=1}^{N_{\text{AP}}} f(t - t^{(p')}) J \sum_{p''=1}^{N_{\text{AP}}} f(t' - t^{(p'')}) \right\rangle \\ &= \frac{J^2}{K} \sum_{N_{\text{AP}}=0}^{\infty} \frac{e^{-\int_0^T ds \Omega_i(s)}}{N_{\text{AP}}!} \int_0^T \cdots \int_0^T \left(\prod_{p=1}^{N_{\text{AP}}} dt^{(p)} \Omega_i(t^{(p)}) \right) \\ &\quad \times \sum_{p'=1}^{N_{\text{AP}}} \sum_{p''=1}^{N_{\text{AP}}} f(t - t^{(p')}) f(t' - t^{(p'')}) \end{aligned}$$

Again, the term $N_{\text{AP}} = 0$ gives no contribution. We continue with a distinction between diagonal ($p' = p''$) and off-diagonal ($p' \neq p''$) terms, evaluating the former first:

$$\begin{aligned} \langle I(t) I(t') \rangle_{p'=p''} &= \frac{J^2}{K} \sum_{N_{\text{AP}}=1}^{\infty} \frac{e^{-\int_0^T ds \Omega_i(s)}}{(N_{\text{AP}} - 1)!} \left(\int_0^T ds \Omega_i(s) \right)^{N_{\text{AP}}-1} \\ &\quad \times \int_0^T dt^{(1)} f(t - t^{(1)}) f(t' - t^{(1)}) \Omega_i(t^{(1)}) \\ &= \frac{J^2}{K} \int_0^T dt^{(1)} f(t - t^{(1)}) f(t' - t^{(1)}) \Omega_i(t^{(1)}), \end{aligned}$$

again using the identity of all N_{AP} terms and the series representation of the exponential function.

Calculating the crosscorrelation of PSCs (off-diagonal terms) involves spike trains with two or more APs. Therefor the double sum contains $N_{\text{AP}}(N_{\text{AP}} - 1)$ terms which, due to the independence of spike times factorize:

$$\begin{aligned} \langle I(t) I(t') \rangle_{p' \neq p''} &= \frac{J^2}{K} \sum_{N_{\text{AP}}=2}^{\infty} \frac{e^{-\int_0^T ds \Omega_i(s)}}{(N_{\text{AP}} - 2)!} \left(\int_0^T ds \Omega_i(s) \right)^{N_{\text{AP}}-2} \int_0^T dt^{(1)} f(t - t^{(1)}) \Omega_i(t^{(1)}) \int_0^T dt^{(2)} f(t' - t^{(2)}) \Omega_i(t^{(2)}) \\ &= \frac{J^2}{K} \int_0^T dt^{(1)} f(t - t^{(1)}) \Omega_i(t^{(1)}) \int_0^T dt^{(2)} f(t' - t^{(2)}) \Omega_i(t^{(2)}) = \langle I(t) \rangle \langle I(t') \rangle \end{aligned}$$

The off-diagonal terms thus cancel the latter term in Eq. A2 and the temporal covariance function of the input current of a single population evaluates to:

$$C_I(t, t') = \langle \delta I(t) \delta I(t') \rangle = \frac{J^2}{K} \Omega_i \int_{-\infty}^{\infty} ds f(t - s) f(t' - s) \quad (\text{A3})$$

3. Covariance of the membrane potential

The membrane potential dynamics are driven by the input current dynamics, derived in App. A 2, which are processed by the LIF-specific membrane potential response function $G(\Delta t) = \frac{1}{\tau_M} e^{-\frac{\Delta t}{\tau_M}}$.

Calculating the crosscorrelation of voltage and current and the autocorrelation of $G(\Delta t)$ beforehand allows the subsequent evaluation of the membrane potential autocorrelation:

$$\begin{aligned} \langle \delta V(t) \delta I(s') \rangle &= \left\langle \int_{-\infty}^{+\infty} ds G(t - s) \delta I(s) \delta I(s') \right\rangle \\ &= \int_{-\infty}^{+\infty} ds G(t - s) C_I(s' - s) \\ G^{(2)}(t) &:= \int_{-\infty}^{+\infty} ds G(s) G(s - t) = \frac{1}{2\tau_M} \exp\left(-\frac{|t|}{\tau_M}\right) \end{aligned}$$

$C_V(t)$ now calculates as:

$$\begin{aligned}
C_V(t) &= \langle \delta V(t) \delta V(0) \rangle = \langle \delta V(t) \int_{-\infty}^{+\infty} ds' G(s') \delta I(-s') \rangle = \\
&= \int_{-\infty}^{+\infty} ds' G(s') \langle \delta V(t) \delta I(-s') \rangle \\
&= \int_{-\infty}^{+\infty} ds' G(s') \int_{-\infty}^{+\infty} ds G(t-s) C_I(-s'-s) \\
&= \int_{-\infty}^{+\infty} ds C_I(s) \int_{-\infty}^{+\infty} ds' G(s') G(s'-s+t) \\
&= \int_{-\infty}^{+\infty} ds C_I(s) G^{(2)}(s-t) \\
&= \frac{\sigma_I^2}{2\tau_M} \int_{-\infty}^{+\infty} ds \exp\left(-\frac{|s|}{\tau_{I_l}}\right) \exp\left(-\frac{|s-t|}{\tau_M}\right),
\end{aligned}$$

using a mono-synaptic kernel, Eq. 3. The integral splits up into three regions: $s < 0$, $0 < s < t$ and $s > t$ and we obtain distinct solutions for the covariance contribution of population l for the case of $\tau_{I_l} \neq \tau_M$:

$$C_{V_l}(\Delta t) = \frac{\sigma_I^2 \tau_{I_l}}{\tau_{I_l}^2 - \tau_M^2} \left[\tau_{I_l} \exp\left(-\frac{|\Delta t|}{\tau_{I_l}}\right) - \tau_M \exp\left(-\frac{|\Delta t|}{\tau_M}\right) \right]$$

and in the case of $\tau_{I_l} = \tau_M$:

$$C_{V_l}(\Delta t) = \frac{\sigma_I^2}{2} \left(1 + \frac{|\Delta t|}{\tau_M} \right) \exp\left(-\frac{|\Delta t|}{\tau_M}\right)$$